3666 *Organometallics* **2009,** *28,* 3666–3672
DOI: 10.1021/om9000617

ORGANOMETALLICS
Article

# Topological Analysis of the Electron Density in the N-Heterocyclic Carbene Triruthenium Cluster $[Ru_3(\mu\text{-}H)_2(\mu_3\text{-}MeImCH)(CO)_9]$ ($Me_2Im$ = 1,3-dimethylimidazol-2-ylidene)

Javier A. Cabeza,*[†] Juan F. Van der Maelen,*[‡] and Santiago García-Granda[‡]

[†]*Departamento de Química Orgánica e Inorgánica-IUQOEM, Universidad de Oviedo-CSIC, E-33071 Oviedo, Spain, and* [‡]*Departamento de Química Física y Analítica-CINN, Universidad de Oviedo-CSIC, E-33071 Oviedo, Spain*

*Received January 27, 2009*

The bonding in the triruthenium dihydrido cluster compound $[Ru_3(\mu\text{-}H)_2(\mu_3\text{-}\kappa^2\text{-}MeImCH)(CO)_9]$ (**1**), which contains a face-capping N-heterocyclic carbene ligand (MeImCH) derived from the activation of two C−H bonds of 1,3-dimethylimidazol-2-ylidene ($Me_2Im$), has been studied from the perspective of the atoms in molecules (AIM) quantum theory. Although the AIM approach recognizes the existence of a bond path in only one of the Ru−Ru edges of complex **1**, i.e., that unbridged by the hydride ligands Ru(1)−Ru(3), the non-negligible values for the delocalization indexes of the hydride-bridged Ru−Ru edges indicate a delocalized kind of metal−metal interaction in these edges. In fact, a multicenter (5c-6e) interaction involving the $Ru_3H_2$ core of the molecule can be proposed. The three-atom C−N−C bridge that spans the Ru(1)−Ru(3) edge of **1** does not delocalize the electronic density of the bridged metal atoms as efficiently as bridges comprising just one atom, such as hydride or CH. The topological parameters of the three Ru−C bonds between the metal atoms and the face-capping NHC ligand are very similar, and they confirm that these interactions are pure $\sigma$-bonds. The analysis of the topological parameters for the bonds of the NHC ligand confirms the presence of $\pi$-electron delocalization within the five-membered ring as well as the existence of some double-bond character in the interaction of the carbene C atom with the adjacent N atoms.



## Introduction

The topological analysis of the electron density, within the framework of the quantum theory of atoms in molecules (AIM),[1] has become a powerful tool for studying chemical bonds. Studies on systems containing light atoms (periods 1−3 of the periodic table) have allowed the establishment of useful links between bonding modes and topological properties of the electron density.[2] However, such links cannot be straightforwardly extended to compounds with transition metal atoms because they display a different and much narrower spectrum of topological indexes.[3−6] Compounds containing bonding interactions between transition metals constitute a particular case, since the AIM approach assigns very little (or none at all) electron density to these bonds and, generally, only finds M−M bond paths when no bridging ligands are present.[3,5] Unfortunately, the number of studies on the electron density topology for cluster compounds with three or more metal−metal interactions between transition metal atoms is still very limited.[3,6] Therefore, more AIM studies on this class of molecules are desirable in order to shed additional light on the bonding between their metal atoms.

On the other hand, although N-heterocyclic carbenes (NHCs) of the imidazol-2-ylidene type have traditionally been considered as pure $\sigma$-donors,[7] recent reports have indicated that they may

*To whom correspondence should be addressed. E-mail: jac@uniovi.es, fvu@uniovi.es.

(1) Bader, R. F. W. *Atoms in Molecules: A Quantum Theory*; Clarendon Press: Oxford, UK, 1990.

(2) (a) Bader, R. F. W. *J. Phys. Chem. A* **1998**, *102*, 731. (b) Koritsanszky, T. S.; Coppens, P. *Chem. Rev.* **2001**, *101*, 1583. (c) Gatti, C. *Z. Kristallogr.* **2005**, *220*, 399.

(3) Macchi, P.; Sironi, A. *Coord. Chem. Rev.* **2003**, *238*, 383.

(4) (a) Farrugia, L. J.; Evans, C.; Tegel, M. *J. Phys. Chem. A* **2006**, *110*, 7952. (b) Farrugia, L. J.; Evans, C.; Lentz, D.; Roemer, M. *J. Am. Chem. Soc.* **2009**, *131*, 1251.

(5) For examples of AIM studies on binuclear complexes, see: (a) Van der Maelen, J. F.; Gutiérrez-Puebla, E.; Monge, A.; García-Granda, S.; Resa, I.; Carmona, E.; Fernández-Díaz, M. T.; McIntyre, G. J.; Pattison, P.; Weber, H. P. *Acta Crystallogr. B* **2007**, *63*, 862. (b) Macchi, P.; Proserpio, D. M.; Sironi, A. *J. Am. Chem. Soc.* **1998**, *120*, 13429. (c) Overgaard, J.; Clausen, H. F.; Platts, J. A.; Iversen, B. B. *J. Am. Chem. Soc.* **2008**, *130*, 3834. (d) Macchi, P.; Garlaschelli, L.; Sironi, A. *J. Am. Chem. Soc.* **2002**, *124*, 14173. (e) Bo, C.; Sarasa, J. P.; Poblet, J. M. *J. Phys. Chem.* **1993**, *97*, 6362. (f) Low, A. A.; Kunze, K. L.; MacDougall, P. J.; Hall, M. B. *Inorg. Chem.* **1991**, *30*, 1079. (g) Bianchi, R.; Gervasio, G.; Marabello, D. *Inorg. Chem.* **2000**, *39*, 2360. (h) Gatti, C.; Lasi, D. *Faraday Discuss* **2007**, *135*, 55.

(6) For examples of topological studies on tri- and polynuclear cluster complexes, see: (a) Gervasio, G.; Bianchi, R; Marabello, D. *Chem. Phys. Lett.* **2005**, *407*, 1. (b) Macchi, P.; Garlaschelli, L.; Martinengo, S.; Sironi, A. *J. Am. Chem. Soc.* **1999**, *121*, 10428. (c) Feliz, M.; Llusar, R.; Andrés, J.; Berski, S.; Silvi, B. *New J. Chem.* **2002**, *26*, 844. (d) Bytheway, I.; Griffith, C. S.; Koutsantonis, G. A.; Skelton, B. W.; White, A. H. *Eur. J. Inorg. Chem.* **2007**, 3240. (e) Niskanen, M.; Hirva, P.; Haukka, M. *J. Chem. Theory Comput.* **2009**, *5*, 1084.

(7) For reviews on NHC−metal complexes, see: (a) Herrmann, W. A.; Köcher, C. *Angew. Chem., Int. Ed.* **1997**, *36*, 2162. (b) Bourissou, D.; Guerret, O.; Gabbaï, F. P.; Bertrand, G. *Chem. Rev.* **2000**, *100*, 39. (c) Alder, R. W.; Blake, M. E.; Chaker, L.; Harvey, J. N.; Paolini, F.; Schütz, J. *Angew. Chem., Int. Ed.* **2004**, *43*, 5896. (d) Arduengo, A. J. *Acc. Chem. Res.* **1999**, *32*, 913. (e) Herrmann, W. A. *Angew. Chem., Int. Ed.* **2002**, *41*, 1290. (f) Special issue: *Coord. Chem. Rev.* **2006**, *251*. (g) Special issue: *J. Organomet. Chem.* **2005**, *690*. (h) Hahn, F. E.; Jahnke, M. C. *Angew. Chem., Int. Ed.* **2008**, *47*, 3122.

 Published on Web 05/14/2009 

also behave as $\pi$-donor or $\pi$-acceptor ligands, depending on the electronic richness of the metal system to which they are attached.[8−11] In this sense, a molecular orbital analysis on the unsaturated 14-e complex $[Ir(^tBu_2Im)_2][PF_6]$ ($^tBu_2Im$ = 1,3-bis-(*tert*-butyl)imidazol-2-ylidene) indicated the existence of a remarkable donation of electron density from a filled $\pi$-type orbital of the NHC ligands to empty d orbitals of the Ir atom ($\pi_{NHC} \rightarrow d_{Ir}$).[9] On the contrary, DFT studies on NHC−Ni and other group 10 metal−NHC complexes have revealed that the M−NHC bond contains an important contribution of back-donation of electron density from filled metal d orbitals to empty $\pi$-type orbitals of the NHC ligand ($d_{Ni} \rightarrow \pi_{NHC}$).[10,11] Spectroscopic and crystallographic studies on various Rh−NHC complexes have also shown that imidazol-2-ylidenes are capable of $\pi$-back-donation and that this interaction may be tuned by changing the $\pi$-acidity of the substituents on the carbene ring.[12] On the other hand, only a couple of AIM studies on metal−NHC complexes have been published to date, both on Cr−NHC compounds, which have shown that $\pi$-electron delocalization is not complete within the ligand ring but slightly hindered instead.[13] However, as far as we are aware, the bonding in NHC−metal complexes on polynuclear compounds has not been previously studied from the AIM point of view.

We now report an AIM topological analysis of the electron density in the NHC triruthenium cluster $[Ru_3(\mu\text{-}H)_2(\mu_3\text{-}MeImCH)(CO)_9]$ (**1**) ($Me_2Im$ = 1,3-dimethylimidazol-2-ylidene),[14] a closed trinuclear cluster that contains one hydride-unbridged and two hydride-bridged Ru−Ru edges and a face-capping ligand with two types of Ru−C bonds (Figure 1), thus allowing interesting comparisons between the topological properties of related but different atom−atom bonding interactions within the same molecule, such as hydride-bridged versus hydride-unbridged Ru−Ru interactions and $Ru-C_{NHC}$ versus other Ru−C interactions.

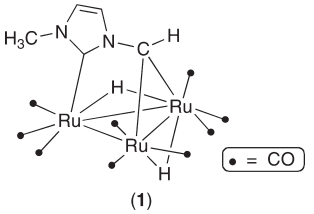

(1)

**Figure 1.** Schematic structure of $[Ru_3(\mu\text{-}H)_2(\mu_3\text{-}MeImCH)(CO)_9]$ (**1**).

## Computational Details

Electronic structure calculations were carried out with the GAUSSIAN03 program package[15] on both the experimental (X-ray diffraction data)[14a] and the theoretically optimized structure of compound **1**. These calculations were performed using both density functional theory (DFT) and *ab initio* perturbation theory (MP) methods. The hybrid[16] B3LYP,[17] B3PW91,[18] and B3P86[19] functionals, together with the Møller-Plesset MP2 and MP3 perturbation theory methods, were tested. The all-electron 6-31G(d,p) basis set was used for C, H, N, and O atoms. The WTBS (well-tempered basis set of Huzinaga and co-workers),[20] 3-21G(d,p), and LanL2DZ basis sets were tested for the Ru atoms. The calculated ground state electronic wave functions, which were found to be stable, were then utilized for further calculations on the topology of the theoretical electron density, within the framework of the AIM approach.[1] These calculations included both local and integral properties and were carried out with the AIM2000 program.[21] The accuracy of the integrated properties was finally set at $1.0 \times 10^{-4}$ (from the Laplacian of the integrated electron density), whereas the accuracy of the local properties was $1.0 \times 10^{-10}$ (from the gradient of the electron density at the bond critical points).

From all the theoretical approaches used (combinations of molecular geometry, calculation method, and basis sets), the B3PW91/6-31G(d,p)/LanL2DZ model was the only one able to render an optimized geometry nearly identical to the experimental one (selected bond distances and angles for both the experimental and the theoretically optimized molecular geometries are included in the Supporting Information, Table S1), and the B3PW91/6-31G(d,p)/WTBS model applied to both the experimental and the optimized geometries was the only one able to find all critical points in the molecule. Therefore, all AIM results described in this work correspond to calculations performed with the B3PW91/6-31G(d,p)/WTBS model on the theoretically optimized geometry obtained with the B3PW91/6-31G(d,p)/LanL2DZ model. No significant differences were found when the experimental or the theoretically optimized geometries were used.

## Results and Discussion

Application of the AIM approach to compound **1** afforded the complete set of bond critical points (bcp's) and ring critical points (rcp's), together with the bond paths (bp's) that connect the bonded atoms through their corresponding bcp's (Figure 2). In addition to the bcp's corresponding to the Ru−C (12 bcp's), Ru−H (4 bcp's), C−O (9 bcp's), C−N (6 bcp's), C−C (1 bcp), and C−H (6 bcp's) bonds, a unique bcp was also found between Ru(1) and Ru(3) atoms. No bcp's

(8) (a) Tonner, R.; Heydenrych, G.; Frenking, G. *Chem. Asian J.* **2007**, *2*, 1555. (b) Cavallo, L.; Correa, A.; Costabile, C.; Jacobsen, H. *J. Organomet. Chem.* **2005**, *690*, 5407. (c) Radius, U.; Bickelhaupt, F. M. *Coord. Chem. Rev.* **2009**, *253*, 678. (d) Jakobsen, R.; Correa, A.; Poater, A.; Costabile, C.; Cavallo, L. *Coord. Chem. Rev.* **2009**, *253*, 687.
(9) Scott, N. M.; Dorta, R.; Stevens, E. D.; Correa, A.; Cavallo, L.; Nolan, S. P. *J. Am. Chem. Soc.* **2005**, *127*, 3516.
(10) Lai, C. L.; Guo, W. H.; Lee, M. T.; Hu, C. H. *J. Organomet. Chem.* **2005**, *690*, 5867.
(11) Radius, U.; Bickelhaupt, F. M. *Organometallics* **2008**, *27*, 3410.
(12) Khramov, D. M.; Lynch, V. M.; Bielawski, C. W. *Organometallics* **2007**, *26*, 6042.
(13) (a) Tafipolsky, M.; Scherer, W.; Öfele, K.; Artus, G.; Pedersen, B.; Herrmann, W. A.; McGrady, G. S. *J. Am. Chem. Soc.* **2002**, *124*, 5865. (b) Scherer, W.; Tafipolsky, M.; Öfele, K. *Inorg. Chim. Acta* **2008**, *361*, 513.
(14) (a) Cabeza, J. A.; del Río, I.; Miguel, D.; Sánchez-Vega, M. G. *Chem. Commun.* **2005**, 3956. (b) Cabeza, J. A.; del Río, I.; Miguel, D.; Pérez-Carreño, E.; Sánchez-Vega, M. G. *Dalton Trans.* **2008**, 1937. (c) Cabeza, J. A.; Pérez-Carreño, E. *Organometallics* **2008**, *27*, 4697.
(15) Frisch, M. J.; Trucks, G. W.; Schlegel, H. B.; Scuseria, G. E.; Robb, M. A.; Cheeseman, J. R.; Montgomery, J. A.Jr.; Vreven, T.; Kudin, K. N.; Burant, J. C.; Millam, J. M.; Iyengar, S. S.; Tomasi, J.; Barone, V.; Mennucci, B.; Cossi, M.; Scalmani, G.; Rega, N.; Petersson, G. A.; Nakatsuji, H.; Hada, M.; Ehara, M.; Toyota, K.; Fukuda, R.; Hasegawa, J.; Ishida, M.; Nakajima, T.; Honda, Y.; Kitao, O.; Nakai, H.; Klene, M.; Li, X.; Knox, J. E.; Hratchian, H. P.; Cross, J. B.; Adamo, C.; Jaramillo, J.; Gomperts, R.; Stratmann, E. R.; Yazyev, O.; Austin, A. J.; Cammi, R.; Pomelli, C.; Ochterski, J. W.; Ayala, P. Y.; Morokuma, K.; Voth, G. A.; Salvador, P.; Dannenberg, J. J.; Zakrzewski, V. G.; Dapprich, S.; Daniels, A. D.; Strain, M. C.; Farkas, O.; Malick, D. K.; Rabuck, A. D.; Raghavachari, K.; Foresman, J. B.; Ortiz, J. V.; Cui, Q.; Baboul, A. G.; Clifford, S.; Cioslowski, J.; Stefanov, B. B.; Liu, G.; Liashenko, A.; Piskorz, P.; Komaromi, I.; Martin, R. L.; Fox, D. J.; Keith, T.; Al-Laham, M. A.; Peng, C. Y.; Nanayakkara, A.; Challacombe, M.; Gill, P. M. W.; Johnson, B.; Chen, W.; Wong, M.; Gonzalez, W. C.; Pople, J. A. *GAUSSIAN-03 (Revision C2)*; Gaussian Inc.: Wallingford, CT, 2004.
(16) Becke, A. D. *J. Chem. Phys.* **1993**, *98*, 5648.
(17) Lee, C.; Yang, W.; Parr, R. G. *Phys. Rev. B* **1988**, *37*, 785.
(18) Perdew, J. P.; Burke, K.; Wang, Y. *Phys. Rev B* **1996**, *54*, 16533.
(19) Perdew, J. P. *Phys. Rev. B* **1986**, *33*, 8822.
(20) (a) Huzinaga, S.; Miguel, B. *Chem. Phys. Lett.* **1990**, *175*, 289. (b) Huzinaga, S.; Klobukowski, M. *Chem. Phys. Lett.* **1993**, *212*, 260.
(21) Biegler-König, F.; Schönbohm, J. *J. Comput. Chem.* **2002**, *23*, 1489.

**Table 1. Atomic Charges for Selected Atoms of 1 Calculated by Different Population Analysis Methods, Using the Theoretical Model B3PW91/6-31G(d,p)/WTBS on the Theoretically Optimized Geometry**

| method | Ru(1) | Ru(2) | Ru(3) | H(100) | H(200) | C(1) | C(2) | C(3) | C(4) | N(1) | N(2) |
|---|---|---|---|---|---|---|---|---|---|---|---|
| Mulliken | 0.569 | 0.514 | 0.642 | −0.235 | −0.236 | 0.171 | 0.043 | 0.024 | −0.540 | −0.311 | −0.454 |
| NBO | 0.533 | 0.513 | 0.568 | −0.285 | −0.282 | 0.138 | 0.082 | 0.092 | −0.626 | −0.398 | −0.391 |
| AIM | 0.620 | 0.711 | 0.596 | −0.257 | −0.235 | 0.658 | 0.754 | 0.702 | −0.235 | −1.051 | −1.053 |

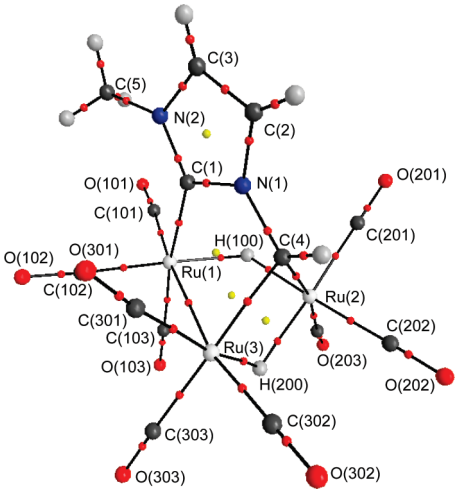


**Figure 2.** Molecular structure of compound **1**, showing the bond paths (black lines) and the bond (small red circles) and ring (small yellow circles) critical points.

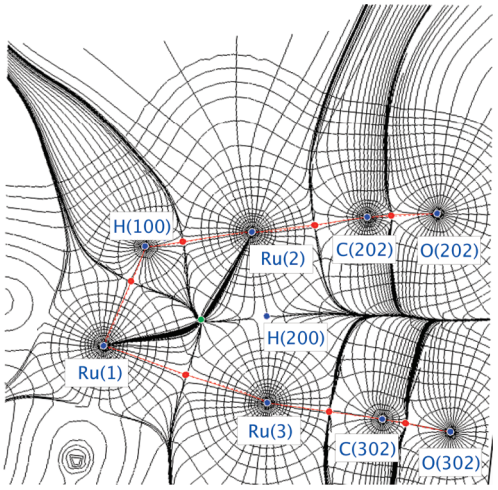


**Figure 3.** Gradient trajectories mapped on a total electron density plot (contour levels at 0.1 e Å$^{-3}$) in the Ru(1)−Ru(2)−Ru(3) plane of **1**, showing the atom basins, bp's (red lines), bcp's (red circles), and a rcp (green circle).

or bp's were found between Ru(1) and Ru(2) or between Ru(2) and Ru(3). Four rcp's were clearly observed, corresponding to the C(1)−N(1)−C(2)−C(3)−N(2), C(1)−N(1)−C(4)−Ru(3)−Ru(1), Ru(1)−H(100)−Ru(2)−H(200)−Ru(3), and Ru(2)−C(4)−Ru(3)−H(200) rings.

Figure 3 displays a gradient trajectory map of the total electron density in the Ru(1)−Ru(2)−Ru(3) plane, showing the bcp and bp between Ru(1) and Ru(3) together with the atomic basins for these and other atoms located in the same plane. Also shown in this figure are both bcp's and bp's found between the hydride ligand H(100), which is contained in that plane, and Ru(1) and Ru(2) metal atoms. Two CO ligands, located nearly in the same plane, are also visible in the plot,

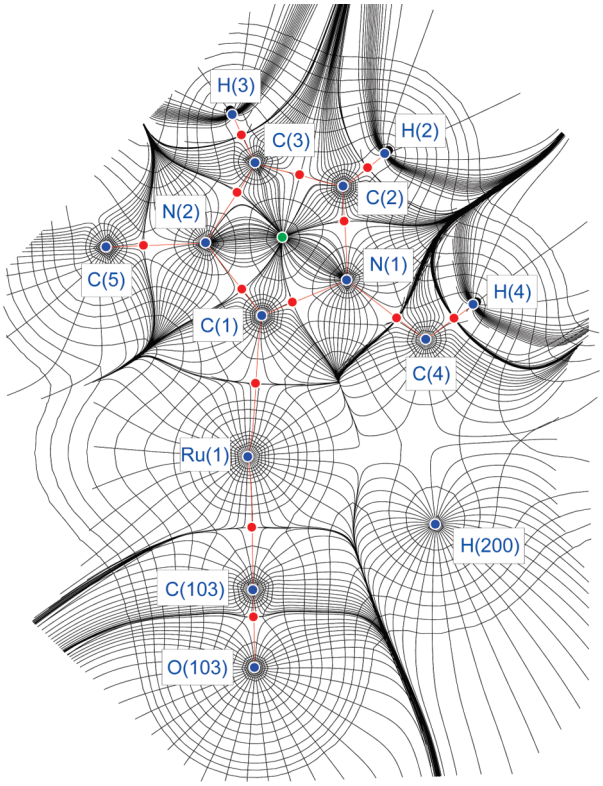


**Figure 4.** Gradient trajectories mapped on a total electron density plot (contour levels at 0.1 e Å$^{-3}$) in the NHC ligand plane of **1**, showing the atom basins, bond paths (red lines), bcp's (red circles), and a rcp (green circle).

including their associated atomic basins, bcp's, and bp's. A projection for the position of the H(200) hydride ligand on this plane is also shown.

A gradient trajectory map of the total electron density in the plane spanned by the MeImCH ligand is depicted in Figure 4. It shows not only the bp's, bcp's, and rcp associated with this ligand, but also the bp's and bcp's of the interactions of Ru(1) with the NHC ligand C(1) atom and with the CO ligand that is *trans* to C(1). The hydride H(200) is also located on the MeImCH ligand plane, but it is not bonded to any of the other atoms of this plane.

Integration of the electron density inside each atomic basin rendered the corresponding atomic electric charges. Table 1 compares AIM charges with those obtained by other commonly used population analysis methods. Whereas Mulliken and natural bond orbital (NBO) population analyses afforded results rather dependent on the theoretical model used (both method and basis set), the AIM approach was very consistent, giving values in the range +0.6 e to +0.7 e for the electric charge of the Ru atoms and −0.2 to −0.3 e for the electric charge of the bridging H atoms. Other atomic charges calculated by means of the AIM methodology, but not shown in Table 1, are +0.7 e to +0.8 e for the carbonyl C atoms and −0.9 to −1.0 e for the O atoms. The electron configuration

**Table 2. Selected Topological Parameters for 1, Calculated Using the Theoretical Model B3PW91/6-31G(d,p)/WTBS on the Theoretically Optimized Geometry**

| bond | $d_{A-B}$ (Å)[b] | $\rho_b$ (e Å$^{-3}$)[c] | $\nabla^2\rho_b$ (e Å$^{-5}$)[d] | $H_b/\rho_b$ (h e$^{-1}$)[e] | $G_b/\rho_b$ (h e$^{-1}$)[f] | $\varepsilon_b$[g] | $\delta$(A−B)[h] |
|---|---|---|---|---|---|---|---|
| Ru(1)−Ru(3) | 2.838 | 0.292 | 0.803 | −0.271 | 0.463 | 0.036 | 0.458 |
| Ru−H[a] | 1.790 | 0.564 | 4.556 | −0.314 | 0.879 | 0.086 | 0.474 |
| Ru−CO[a] | 1.931 | 0.951 | 13.304 | −0.393 | 1.372 | 0.030 | 1.089 |
| Ru(1)−C(1) | 2.084 | 0.745 | 7.145 | −0.304 | 0.976 | 0.081 | 0.764 |
| Ru(2)−C(4) | 2.131 | 0.712 | 4.793 | −0.307 | 0.778 | 0.069 | 0.760 |
| Ru(3)−C(4) | 2.122 | 0.725 | 5.111 | −0.313 | 0.806 | 0.051 | 0.757 |
| N(1)−C(1) | 1.355 | 2.201 | −17.695 | −1.645 | 1.082 | 0.162 | 1.131 |
| N(1)−C(2) | 1.385 | 2.035 | −17.851 | −1.535 | 0.921 | 0.150 | 1.055 |
| N(1)−C(4) | 1.459 | 1.693 | −13.348 | −1.386 | 0.834 | 0.060 | 0.906 |
| N(2)−C(1) | 1.354 | 2.162 | −15.295 | −1.632 | 1.136 | 0.181 | 1.143 |
| N(2)−C(3) | 1.385 | 2.018 | −15.789 | −1.551 | 1.004 | 0.140 | 1.045 |
| C(2)−C(3) | 1.341 | 2.330 | −24.314 | −1.112 | 0.381 | 0.376 | 1.380 |
| C−O[a] | 1.144 | 2.925 | 15.176 | −1.495 | 1.858 | 0.002 | 1.789 |

[a] Average values (equal figures up to the second decimal digit). [b] Bond path length. [c] Electron density at the bcp. [d] Laplacian of the electron density at the bcp. [e] Total energy density ratio at the bcp. [f] Kinetic energy density ratio at the bcp. [g] Ellipticity at the bcp. [h] Delocalization index.

**Table 3. Delocalization Indexes for Selected Nonbonding Interactions involving Ru Atoms in 1, Calculated Using the Theoretical Model B3PW91/6-31G(d,p)/WTBS on the Theoretically Optimized Geometry**

| | Ru(1)···Ru(2) | Ru(2)···Ru(3) | Ru···O$_{CO}$[a] | Ru(1)···N(1,2)[a] | Ru(2,3)···N(1)[a] |
|---|---|---|---|---|---|
| $\delta$(A···B) | 0.169 | 0.246 | 0.202 | 0.055 | 0.052 |

[a] Average value (equal figures up to the first significant digit).



obtained from the NBO analysis for the Ru atoms was [core]5s$^{0.4}$4d$^{7.1}$, with other noncore orbitals contributing less than 0.1 e, while the electron configuration obtained for the bridging H atoms was 1s$^{1.3}$.

There are several local (i.e., calculated at the bcp) and integral (i.e., calculated over the atomic basin) topological properties of the electron density that have been successfully used to analyze the bonding in molecules containing transition metals. Among the former, the electron density ($\rho_b$), the ellipticity ($\varepsilon_b$), the Laplacian of the electron density ($\nabla^2\rho_b$), the kinetic energy density ratio ($G_b/\rho_b$), and the total energy density ratio ($H_b/\rho_b$), with $H_b(r) = G_b(r) + V_b(r)$ and $1/4\nabla^2\rho_b(r) = 2G_b(r) + V_b(r)$, where $V_b(r)$ is the potential energy density, are by far the most relevant.[1−6] On the other hand, the delocalization index $\delta$ (A−B), which is an integral property, indicates the number of electron pairs shared by atoms A and B.[2c,3,22] Values of these topological properties, for selected bonds of molecule **1**, are collected in Table 2.

**Ru−Ru and Ru−H Interactions.** For the Ru(1)−Ru(3) interaction, the value of the electron density at the bcp (0.292 e Å$^{-3}$), the positive but small value of the Laplacian at the bcp (0.803 e Å$^{-5}$), the positive but less than unity value of $G_b/\rho_b$ (0.463 h e$^{-1}$), and the small negative value of $H_b/\rho_b$ (−0.271 h e$^{-1}$) indicate that the Ru−Ru bond in **1** is a typical open-shell metal−metal interaction, intermediate between pure covalent and pure ionic bonds between nonmetal atoms. These values are comparable to those previously found, from both experimental and theoretical electron densities, for other unbridged metal−metal bonds, such as the Zn−Zn bond in [Zn$_2$($\eta^5$-C$_5$Me$_5$)$_2$],[5a] the Co−Co bonds in several compounds,[5b−5d] and the Ru−Ru bonds in [Ru$_2$(formamidinate)$_4$],[5h] [Ru(CO)$_4$]$_n$,[6e] and [Ru$_3$(CO)$_{12}$].[6a] For instance, in the latter compound, which contains three Ru−Ru bonds, an average value of 0.215 e Å$^{-3}$ was found for $\rho_b$, with an average ellipticity at the bcp of 0.022 and an average value of 0.791 h e$^{-1}$ for $G_b/\rho_b$. Nevertheless, the integrated topological properties are more useful than the local topological properties for characterizing metal−metal bonds.[2c,5h] In this sense, the delocalization index, $\delta$(Ru−Ru), is one of the most powerful tools, and the calculated value for the Ru(1)−Ru(3) interaction of **1** (0.458) suggests that there is about half an electron pair shared by the two Ru atoms (but see below). On the contrary, for the compound [Ru$_2$(formamidinate)$_4$], where a localized Ru−Ru bond is clearly present, as evidenced from source function (SF) calculations,[5h] a value of 1.316 is obtained for this index, with $\rho_b$ = 0.494 e Å$^{-3}$ and $\nabla^2\rho_b$ = 1.588 e Å$^{-5}$, almost double the values found for **1**. In addition, the integrated electron density over the whole interatomic surface, $\oint_{A\cap B}\rho$, which is an integral property related to the bond strength, gives a value of 1.36 e Å$^{-1}$ for the Ru(1)−Ru(3) bond in **1**, smaller than but comparable in magnitude to that of pure covalent bonds, such as the C−C bond of ethane (2.16 e Å$^{-1}$),[3] despite the fact that $\rho_b$ is 1 order of magnitude lower for the Ru(1)−Ru(3) bond than for a pure covalent bond between nonmetal atoms (Table 2).

No bcp's or bp's were found for the hydride-bridged Ru(1)···Ru(2) or Ru(2)···Ru(3) interactions. However, their delocalization indexes, $\delta$(Ru···Ru), are not negligible at all (Table 3) but comparable in magnitude to, or even greater than, other values found for ligand-bridged metal−metal interactions in several organometallic compounds,[2c,3,5e] being also comparable to the delocalization indexes computed, for instance, for the Co−Co and B−C unbridged interactions of [Co$_2$(CO)$_8$] (0.46)[5f] and H$_3$BCO (0.50),[3] respectively. Curiously enough, the Ru(1)−Ru(3) edge of **1**, although it is not bridged by a hydride ligand, is bridged by the face-capping MeImCH ligand, but the C(1)−N(1)−C(4) bridge does not seem to favor the electronic communication between Ru(1) and Ru(3) atoms. Therefore, the delocalization index is an important property to easily recognize ligand-bridged metal−metal interactions, but, unfortunately, it is only directly accessible from theoretical and not from experimental electron densities,[2c,3] for which the source function may be a useful alternative.[5h]

(22) Bader, R. F. W.; Stephens, M. E. *J. Am. Chem. Soc.* **1975**, *97*, 7391.

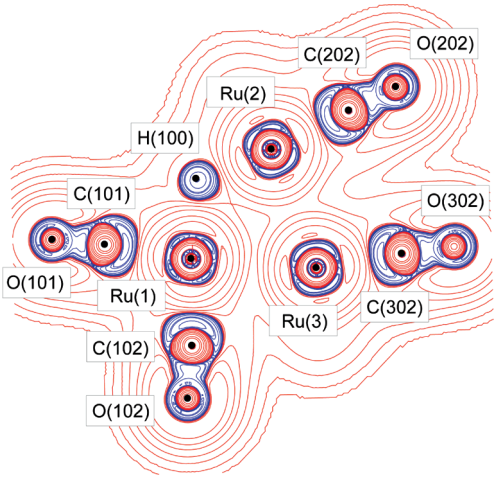


**Figure 5.** Laplacian of the electron density in the Ru(1)−Ru(2)−Ru(3) plane of **1** (contour levels at 0.0 and ±(1,2,4,8) × $10^n$ e Å$^{-5}$, with $n$ ranging from +3 to −3). Blue and red lines represent negative and positive values, respectively.

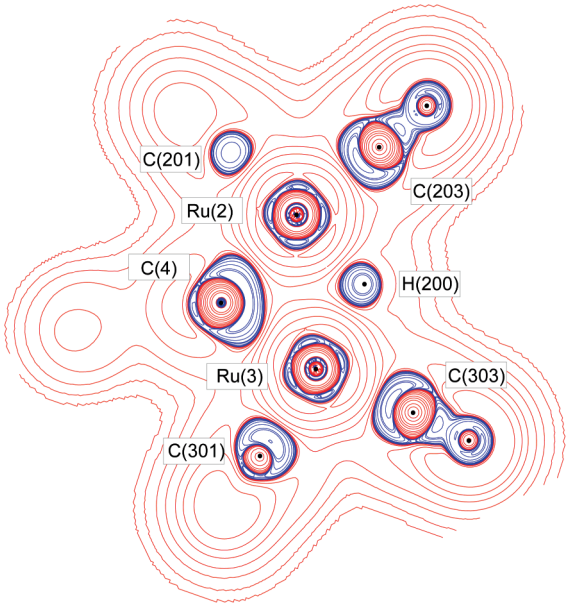


**Figure 6.** Laplacian of the electron density in the Ru(2)−C(4)−Ru(3) plane of **1** (contour levels at 0.0 and ±(1,2,4,8) × $10^n$ e Å$^{-5}$, with $n$ ranging from +3 to −3). Blue and red lines represent negative and positive values, respectively.

Previous topological studies on complexes containing M−H bonds (M = transition metal) are very scarce,[23,24] and even rarer are topological studies on di- or polynuclear transition metal complexes containing bridging hydride ligands, which, to the best of our knowledge, are restricted to only one example that studies the first-row transition metal complex $[Cr_2(\mu\text{-H})(CO)_{10}]^-$.[24] An average value of 1.348 e Å$^{-1}$ for the integrated electron density over each of the Ru−H interatomic surfaces of **1** indicates that the strength of these bonds is comparable to that of pure covalent single bonds between nonmetal atoms.[3] Additionally, Table 2 shows that the delocalization index $\delta$(Ru−H) for **1** (0.474) is higher than $\delta$(Cr−H) for $[Cr_2(\mu\text{-H})(CO)_{10}]^-$ (0.38) and only marginally lower than $\delta$(Cr−H) for the terminal hydride complex $[CrH(CO)_5]^-$ (0.59).[24] Rather interestingly, the calculated $\delta$(Ru−H) values suggest that about half an electron pair is shared in each of the four Ru−H bonds, just as in the Ru(1)−Ru(3) bond, despite the fact that the topology of both kinds of bonds is quite different, as reflected by their local topological parameters (Table 2).

No bending was found in the bond paths of Ru(1)−Ru(3) or Ru−H interactions. In addition, the values of the computed bond path lengths (Table 2) are very similar to the interatomic distances obtained from the X-ray diffraction data[14a] and also from the theoretically optimized geometry (Supporting Information, Table S1). These facts, added to the very low ellipticities of these bonds, which are related to the bond symmetry, allow us to conclude that Ru(1)−Ru(3) and Ru−H interactions in **1** are nearly straight bond paths. On the other hand, the large numerical differences between the density values at bcp's and the integrated electron densities along the bond paths suggest that both bonds are rather diffuse.

The nature of the bonding in the $Ru_3H_2$ part of the molecule may also be appreciated in the graphical representations of the Laplacian of the electron density in the Ru(1)−Ru(2)−Ru(3) (Figure 5) and Ru(2)−C(4)−Ru(3) (Figure 6) planes of the molecule. The bridging hydrogen H(100) is surrounded by a unique valence shell charge concentration (VSCC, one maximum is found in the Laplacian), polarized toward the midpoint of the Ru(1)−Ru(2) edge (Figure 5). A similar feature is observed for the VSCC of H(200), which is also polarized, in this case toward the midpoint of the Ru(2)−Ru(3) edge (Figure 6). In both cases the polarization is small, giving slightly more positive values for the Laplacian in the four Ru−H bcp's (Table 2) than those expected in the absence of such polarization. These graphs also show that the VSCCs of the carbonyl C atoms are directed toward the Ru atoms to which they are bonded and also that the VSCCs of the latter have a pseudocubic shape due to their pseudo-octahedral coordination, slightly perturbed by the presence of the two off-axis hydrides. In Figure 6, the VSCCs of the bridging C(4) atom pointing toward both Ru(2) and Ru(3) atoms can also be observed, a similar situation to that previously observed for the C atoms of carbonyl ligands bridging two Co atoms, although in the present case two maxima of the Laplacian are observed for the two bonds involved, instead of one.[3]

Then, by summarizing all these features, it can be concluded that there exists a multicenter (5c-6e) interaction involving the three ruthenium atoms and the two hydrides of compound **1**. In fact, by adding up the five $\delta$(A−B) values for the bonding interactions and the two $\delta$(Ru···Ru) values for the non-bonding interactions in the Ru(1)−H(100)−Ru(2)−H(200)−Ru(3) ring, a total of 2.769 electron pairs is obtained, which is approximately the same as if three Ru−Ru bonds were present, each one with a bond order of about unity.

**Ru−CO and Ru−$C_{NHC}$ Interactions.** The values of the topological indexes included in Table 2 for the Ru−CO bonds of **1** are similar to those found in the literature for other metal−CO bonds.[3,4,5b−5d,6a,6b,23−28] These bonds are

(23) Abramov, Y. A.; Brammer, L.; Klooster, W. T; Bullock, R. M. *Inorg. Chem.* **1998**, *37*, 6317.
(24) Macchi, P.; Donghi, D.; Sironi, A. *J. Am. Chem. Soc.* **2005**, *127*, 16494.
(25) Pillet, S.; Wu, G.; Kulsomphob, V.; Harvey, B. G.; Ernst, R. D.; Coppens, P. *J. Am. Chem. Soc.* **2003**, *125*, 1937.
(26) Stash, A. I.; Tanaka, K.; Shiozawa, K.; Makino, H.; Tsirelson, V. G. *Acta Crystallogr. B* **2005**, *61*, 418.
(27) Wang, C.-C.; Wang, Y.; Liu, H.-J.; Lin, K.-J.; Chou, L.-K.; Chan, K.-S. *J. Phys. Chem. A* **1997**, *101*, 8887.
(28) Bianchi, R.; Gervasio, G.; Marabello, D. *Acta Crystallogr. B* **2001**, *57*, 638.

characterized by a $\rho_b$ value close to 1 e Å$^{-3}$, higher than those of metal−metal bonds but lower than those of pure covalent single bonds between nonmetal atoms, a large positive value of $\nabla^2\rho_b$, a value of around unity for $G_b/\rho_b$, and a small negative value for $H_b/\rho_b$. In addition, a formal bond order of 1 may be inferred from the delocalization index value, $\delta$(Ru−C), also shown in Table 2. Detecting the $\pi$-back-donation from the metal to the CO ligand is difficult because the cylindrical symmetry of the density along the M−CO bond path hides any trace of preferential accumulation planes. Moreover, charges are sensitive to many different effects, like the polarity of the M−CO bond, and therefore cannot be taken as indicators of back-donation. The most reasonable sign of $\pi$-back-donation comes from the M···O$_{CO}$ delocalization index, $\delta$(M···O$_{CO}$), because $\pi$-back-donation involves significant M···O$_{CO}$ interaction.[3] In fact, values of $\delta$(Cu···O$_{CO}$) and $\delta$(B···O$_{CO}$) for $[Cu(CO)_2]^+$ and $H_3BCO$, in which no $\pi$-back-donation exists, are very low, 0.09 and 0.04, respectively, while $\delta$(M···O$_{CO}$) for Fe, Co, and Ni carbonyl complexes are much higher, ranging from 0.15 to 0.25.[3] The $\delta$(Ru···O$_{CO}$) values for complex **1** are precisely within this range (0.202 on average, see Table 3), clearly indicating the presence of $\pi$-back-donation. These results are also confirmed by the topological indexes of the C−O bonds of **1** (Table 2), which are consistent with a weakening of the C−O bonding (larger $d_{C-O}$ and smaller density, Laplacian, $|H_b/\rho_b|$, and $G_b/\rho_b$) in comparison with that of free CO or $H_3BCO$.

Regarding the bonds between Ru atoms and the face-capping NHC ligand, it is quite interesting to compare the Ru(1)−C(1) bond, which involves the carbene C(1) atom, with the two almost equivalent Ru(2)−C(4) and Ru(3)−C(4) bonds, which involve the sp$^3$-hybridized C(4) atom. Although values for the local topological properties of these three bonds are not exactly equal, they are very similar indeed (Table 2). These values are also comparable to those obtained from both experimental and theoretical electron densities for the Cr−C$_{carbene}$ bonds of the Fischer-type carbene complexes [Cr{C(OMe)C≡CPh}(CO)$_5$] and [Cr{C(NH$_2$)CH$_3$}(CO)$_5$],[27] the NHC derivative [Cr(Me$_2$Im)(CO)$_5$],[13] and the Co−C$_{carbene}$ bond of [Co$_2$($\mu$-$\eta^1$-C$_4$O$_2$H$_2$)($\mu$-CO)(CO)$_6$].[28] For instance, the ellipticity at the bcp of the Cr−C$_{carbene}$ bond of [Cr(Me$_2$Im)(CO)$_5$], which has the same NHC ligand as **1**, was found to be between 0.04 (calculated) and 0.08 (experimental),[13a] very close to the value found for **1** (0.081), a feature also shown by the Laplacian (between 6.0 and 6.7 e Å$^{-5}$ for the Cr complex vs 7.1 e Å$^{-5}$ for **1**), whereas $\rho_b$ (0.52 vs 0.745 e Å$^{-3}$) is not so close for both systems, which is in line with the different values for the NBO C$_{carbene}$ charges calculated for both compounds (0.24 vs 0.138, Table 1). On the other hand, calculated charges for the ligand N atoms are nearly the same (−0.37 vs −0.39). The delocalization indexes computed for the three Ru−C$_{NHC}$ interactions in **1** indicate that about 0.8 electron pair is shared between each pair of bonded atoms, a value clearly greater than those found for the Ru(1)−Ru(3) and Ru−H bonds, but smaller than those of the Ru−CO bonds. In addition, the integrated electron densities calculated over each of the three Ru−C$_{NHC}$ interatomic surfaces are also very similar, 1.811 e Å$^{-1}$ for Ru(1)−C(1), 1.743 e Å$^{-1}$ for Ru(2)−C(4), and 1.840 e Å$^{-1}$ for Ru(3)−C(4), and their values suggest that the strength of these bonds is comparable to those of pure covalent single bonds between nonmetal atoms.[3] Figures 6 and 7 clearly show that, as expected, the VSCCs of C(1) and the bridging C(4) atom are distorted toward the metal atoms to which they are attached.

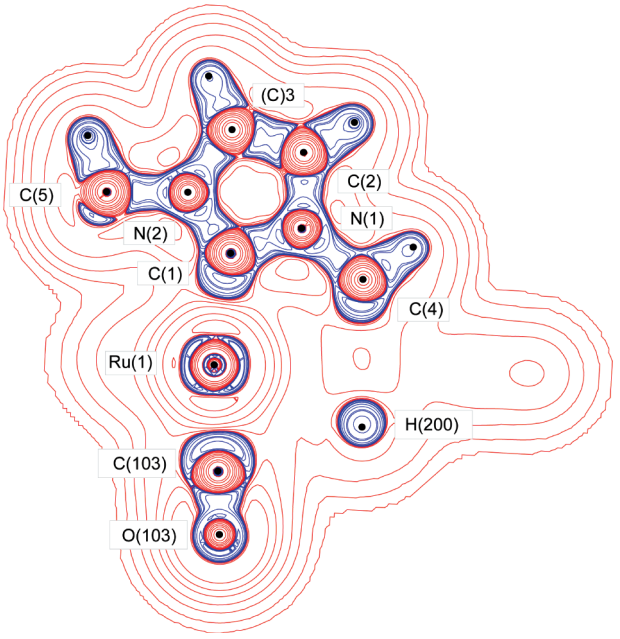


**Figure 7.** Laplacian of the electron density in the N(1)−C(1)−N(2) plane of **1** (contour levels at 0.0 and ±(1,2,4,8) × 10$^n$ e Å$^{-5}$, with $n$ ranging from +3 to −3). Blue and red lines represent negative and positive values, respectively.

As discussed above, the value of $\delta$(M···O$_{CO}$) is indicative of the presence or absence of $\pi$-back-bonding in M−CO bonds. Hence, delocalization indexes for the Ru(1)···N(1) and Ru(1)···N(2) interactions were calculated in an attempt to establish the presence or absence of any kind of $\pi$-bonding in the Ru(1)−C(1) bond. As shown in Table 3, these values are very small and nearly equal to those found for the delocalization indexes of the Ru(2)···N(1) and Ru(3)···N(1) interactions, for which $\pi$-bonding is obviously not possible. Therefore, the imidazol-2-ylidene NHC fragment of the face-capping MeImCH ligand of complex **1** behaves as a pure $\sigma$-donor.

**C−C and C−N Interactions within the Bridging NHC Ligand.** The main features of the bonding between the atoms of the NHC ligand are collected in Tables 1 and 2 and may be graphically visualized in Figures 4 and 7. The gradient trajectory map depicted in Figure 4 shows the bcp's and bp's found between the atoms of the NHC ligand as well as their atomic basins. As expected for polar bonds, with the only exception of the C(2)−C(3) bond, the positions of the bcp's are not symmetrical but shifted toward the less electronegative atom (A−bcp and bcp−B distances for all A−B bonds of **1** are collected in Table S2 of the Supporting Information). Atomic charges calculated for the NHC ligand atoms, obtained from the integration of the electron density inside each atomic basin, are collected in Table 1. While the AIM charges of all carbon atoms are positive, except for the exocyclic carbon atom C(4), with similar values around +0.7 e, the charges of the nitrogen atoms N(1) and N(2) are negative, −1.051 and −1.053 e, respectively. In particular, the charge of the carbene carbon C(1) is +0.658 e, the least positive of the three ring carbon atoms. The map of the Laplacian of the electron density in the NHC ligand plane (Figure 7) shows that every bcp between nonmetal atoms is located in a negative region of the Laplacian, a very much expected result, while the bcp's of metal−ligand and metal−metal interactions are located in positive regions.

The values of the topological parameters of the NHC ligand bonds (Table 2) are all typical for covalent bonds between nonmetal atoms with some degree of delocalization.[2] It is interesting to compare the topological parameters of N(1)−C(1) and N(2)−C(1) bonds with those of the N(1)−C(2) and N(2)−C(3) bonds. The former have high values of the density at the bcp, $\rho_b$, moderate values of the ellipticity, $\varepsilon_b$, and delocalization indexes $\delta$(N−C) slightly greater than unity, whereas the N(1)−C(2) and N(2)−C(3) bonds present slightly smaller values for these three parameters. These results indicate that the N(1)−C(1) and N(2)−C(1) bonds have a slightly greater character of double bonds than the N(1)−C(2) and N(2)−C(3) bonds. This is also corroborated by the bond path lengths, which are slightly shorter for the former. These facts support the previous proposal that the unsaturation of the carbene C atom of an NHC is alleviated by $\pi$-donation of electron density from the filled p−$\pi$ orbitals of the N atoms to the empty p−$\pi$ orbital of the carbene carbon.[7] The highest $\rho_b$ value for the NHC ligand of **1** (in fact, for the whole molecule except for the C−O bonds) belongs to the C(2)−C(3) bond, which also possesses the most negative value for the Laplacian at the bcp, the highest ellipticity, and also the highest delocalization index, values that are consistent with a formal double bond with a certain degree of delocalization within the five-membered ring. Conversely, the topological properties of the N(1)−C(4) bond are prototypical for a formal single covalent bond. For the sake of comparison, for an isolated imidazole molecule, the average values of $\rho_b$ and $\nabla^2\rho_b$ for the four C−N bonds are 2.20 e Å$^{-3}$ and −17.4 e Å$^{-5}$, respectively,[2b] whereas for the carbene complex [Cr(Me$_2$Im)(CO)$_5$],[13a] the respective values are 1.97 e Å$^{-3}$ and −15.2 e Å$^{-5}$ for the C$_{carbene}$−N bonds, 1.95 e Å$^{-3}$ and −15.5 e Å$^{-5}$ for the N−C bonds, and 2.14 e Å$^{-3}$ and −20.3 e Å$^{-5}$ for the C−C bond, the ellipticities of these bonds being 0.13, 0.21, and 0.40, respectively, also very similar to those calculated for these bonds in compound **1** (Table 2).

An alternative way to quantify the electronic delocalization within this kind of ligands is to compute the component of the atomic quadrupole moment perpendicular to the ligand plane, which is the charge-density analogue of $p_\pi$ occupation.[13a,13b] As revealed by the analysis of the traceless quadrupole moment tensor for the carbene carbon in **1**, the charge density is mainly concentrated along the $z$ axis (perpendicular to the ring plane), with the $Q_{zz}$ value being negative ($Q_{zz}$ = −2.370 au, $Q_{xx}$ = 0.280 au; the $x$ axis coincides with the C$_{carbene}$−Ru bond). These values compare well to those reported for [Cr(Me$_2$Im)(CO)$_5$] ($Q_{zz}$ = −2.250 au, $Q_{xx}$ = 0.005 au) and [Cr(Me$_2$Pz)(CO)$_5$] (Me$_2$Pz = 1,2-dimethylpyrazol-3-ylidene) ($Q_{zz}$ = −2.113 au, $Q_{xx}$ = −0.134 au).[13a] All these features are characteristic of slightly hindered $\pi$-electron delocalization within the five-membered ring of the NHC ligands.[13a]

## Conclusions

Although the AIM theory recognizes the existence of a bond path in only one of the three Ru−Ru edges of complex **1**, i.e., that unbridged by the hydride ligands, Ru(1)−Ru(3), the non-negligible values obtained for the delocalization indexes of the two hydride-bridged Ru−Ru edges suggest a delocalized kind of interaction in the central part of the molecule. Consequently, a multicenter (5c-6e) interaction involving the three ruthenium atoms and the two hydrides of compound **1** is here proposed. The three-atom C−N−C bridge that spans the Ru(1)−Ru(3) edge of cluster **1** is not as efficient as bridges comprising one atom (hydride and/or CH) in order to delocalize the electronic density of the bridged metal atoms.

All topological parameters calculated for the three existing Ru−C bonds between the metal atoms and the face-capping NHC ligand are very similar, and they confirm that these interactions are pure $\sigma$-bonds. Therefore, there is no $\pi$-bonding in the Ru−C$_{carbene}$ bond of compound **1**.

The analysis of the topological parameters of the NHC ligand bonds confirms the presence of hindered $\pi$-electron delocalization within the five-membered ring and the existence of some double-bond character in the interaction of the carbene C atom with the adjacent N atoms. Thus, the AIM theory supports the previous proposal that the unsaturation of the carbene C atom of an imidazol-2-ylidene-type NHC ligand is alleviated by donation of electron density from the filled p−$\pi$ orbitals of the N atoms to the empty p−$\pi$ orbital of the carbene carbon.

Finally, it should be mentioned that the application of AIM quantum theory methods to the treatment of bonding in transition metal cluster complexes has hitherto been little studied. In addition, to the best of our knowledge, no previous reports dealing with the bonding between NHC ligands and transition metal cluster complexes have appeared in the literature. The present work contributes to shed more light on these two areas.

**Acknowledgment.** This work has been supported by the European Union (FEDER grants) and the Spanish MCINN (projects CTQ2007-60865, MAT2006-01997, and CSD2006-00015). We also thank the referees of this paper, whose valuable comments and suggestions improved the original manuscript.

**Supporting Information Available:** Tables of interatomic distances and angles for the experimental (X-ray diffraction) and theoretically optimized geometry of compound **1**, and distances from bcp's to bonded atoms. This material is available free of charge via the Internet at http://pubs.acs.org.